Rotorcraft's 'Multiblade' Modelling for an Autogyro

[1,2]**S. A. Shah,** [3]**D. G. Thomson**

[1]Postgraduate Researcher, Aerospace Division, School of Science and Engineering, University of Glasgow, Glasgow G12 8QQ, United Kingdom

[2]Lecturer, Universiti Kuala Lumpur - MIAT, Lot 2891, Jalan Jenderam Hulu, Dengkil, 43800 Selangor, Malaysia

[3]Senior Lecturer, Aerospace Division, School of Science and Engineering, University of Glasgow, Glasgow G12 8QQ, United Kingdom

shahrul@unikl.edu.my

*Research paper

ABSTRACT

The University of Glasgow has involved in the research study of autogyro's flight mechanics for more than 15 years. This paper is giving an overview of the mathematical model development of a light autogyro, emphasising on the rotor model that employs one of the existing helicopter modelling approaches developed at Glasgow, the 'multiblade' or the 'rotor-disc' modelling approach. The method is based on the analytical calculation approach of the rotor loads, in which the elemental load of the blade is analytically integrated over the whole span of the blade and forms an approximation of the rotor 'disc' loads as a whole. In this approach, the blade is considered as a simplified aerofoil with an average lift and drag coefficients, without capturing the aerodynamic details of each geometrical point of the blade. Validation of this model is done by comparing the trim simulation results against the existing trim flight test data acquired from the previous research of the same autogyro. There are good agreements between the simulation results and the flight test data for most of the flight parameters, not as precise as the other previously used 'individual-blade' model approach, but are acceptable due to the advantage this multiblade approach has as a trade-off between the fast computer processing time and the accuracy of predictions. This autogyro's multiblade modelling approach is expected to be used in more autogyro applications where the advantages of this approach are required the most.

Keywords: Autogyro, rotorcraft, multiblade, rotor-disc, flight dynamics.

INTRODUCTION

An autogyro (see Fig.1) is a unique type of rotorcraft vehicle that flies with an unpowered rotor, based on a physics principle called *autorotation*. In this condition, the rotor turns freely due to the lift force created by the rotor blades with the function of the aircraft's forward velocity in maintaining the aircraft in airborne. For a helicopter, the autorotation is a special condition held on the vehicle during an emergency of engine breakdown. In this situation, the rotor shaft is disconnected from the engine governor and the vehicle is forced into the state of autorotation to lead the helicopter for a safety landing. However, for an autogyro, the autorotation is a normal flying state of the vehicle in which, the rotor blade turns due to external aerodynamic forces without the existence of the shaft torque from the engine governor. This unique flying principle of an autogyro is explained by Leishman (2006).

There has been significant interest in this type of vehicle for the last ten years especially in the Europe, not just in recreational and hobby flying but also interest of using it in civil aviation like helicopters. This is due to one obvious advantage an autogyro has over a helicopter, which

is low operating cost including the maintenance. The low-speed flight capability this vehicle has is also seen as an advantage over a fixed wing aircraft and could be utilised for missions such as aerial surveillance for the law enforcement, including search and rescue missions.

However, there are also a significant amount of concern regarding bad safety records of autogyros. In the United Kingdom for instance, the statistics of accident rate involving autogyros in 10 years time (1992-2001) was quite alarming (Anon., 2002). Dynamic instability related issues, or the so-called *pitch instability* to be more specific (instability in longitudinal mode), are the most highlighted cause of these incidents, which also resulted to poor handling qualities of the vehicle (Bagiev and Thomson, 2009, 2010). One important factor that is affecting the longitudinal stability of an autogyro in autorotative forward flight is the rotorspeed. Since an autogyro flies with the rotor disc pitched backwards, maintaining an upward airflow through the disc is crucial. The disc angle of attack must remain positive in all manoeuvres for all speed ranges. Over-speed the blade rotation will cause structural failure on the blade due to excessive lift force and flapping. Under-speed the blade rotation will likely unload the rotor disc and may lead to a stall. Due to this factor, it takes quite a significant amount of flying hours for an experienced pilot to familiarise themselves flying an autogyro as compared to an aeroplane or a helicopter.

The development of an autogyro mathematical model usually started with the consideration of an existing rotorcraft model, due to the similarities an autogyro have as a simple rotorcraft with rotating blades that act on the same principle as the main rotor of a helicopter. In specific, the mathematical model of the light autogyro developed in this research is based on the existing conventional helicopter's '*multiblade*' rotor calculation approach developed at the University of Glasgow (Thomson, 1992). The similar approach has also been widely used in many helicopter flight dynamic studies and also generally described by Padfield (2008). In this multiblade approach, the rotor loads are calculated by considering the external loads at a particular point on the blade element, and analytically integrate the elemental loads over the whole span of the blade, which form into average loads that approximate the entire rotor as a "disc". Assumptions are made in a way that the autogyro's rigid body dynamics are influenced mainly by the steady component of the rotor forces. Under this circumstance, the rotor disc forces are calculated as having steady values for the entire disc, even though the elemental velocities and accelerations actually varies along with both, radial and azimuth position of the blades.

In contrary to that, another modelling approach called the '*individual-blade*' model, implements a more precise and extensive approach, where the uncertain periodicity of the rotating blade is accounted (Houston, 1991). In this approach, each blade is divided into a number of elements per blade, where changes of elemental velocities and accelerations are also modelled in detail. These changes in velocities and accelerations with both radial and azimuth position of the blade resulted in unsteady loads along the blade rotation. Furthermore, the integration of rotor loads are made numerically, which make the simulations of the entire model to be more precise, with

a higher fidelity in predictions, but cumbersome and complex concerning the processor run-time and hardware. In contrast, the simulation of a multiblade model is faster and less complicated for larger scale applications, where higher in accuracy is less of a priory.

DESCRIPTION OF THE MATHEMATICAL MODEL

The mathematical model of the vehicle starts with the implementation of the equations of motion of the autogyro's airframe, with the assumption that the whole airframe is a rigid body, centred at the centre of gravity (c.g.), as shown in Fig.2. The translational and angular velocities of the autogyro's c.g. in the body-fixed axes set are defined as

$$\boldsymbol{v}_{cg}^{b} = \begin{bmatrix} U & V & W \end{bmatrix}^{T} \tag{1}$$

$$\boldsymbol{\omega}_{b} = \begin{bmatrix} P & Q & R \end{bmatrix}^{T} \tag{2}$$

while, the accelerations of the c.g. in the body axes is defined as

$$\boldsymbol{a}_{cg}^{b} = \begin{bmatrix} (\dot{U} + WQ - RV) & (\dot{V} + RU - PW) & (\dot{W} + PV - QU) \end{bmatrix}^{T} \tag{3}$$

$$\boldsymbol{\alpha}_{b} = \begin{bmatrix} \dot{P} & \dot{Q} & \dot{R} \end{bmatrix}^{T} \tag{4}$$

According to Eqs.(1) - (4), $\boldsymbol{v}_{cg}^{b}$ and $\boldsymbol{\omega}_{b}$ are the translational and angular velocity vectors, while $\boldsymbol{a}_{cg}^{b}$ and $\boldsymbol{\alpha}_{b}$ are the translational and angular accelerations of the autogyro in the body axes orientation.

The light autogyro used in the research is the University of Glasgow's Montgomerie-Parsons G-UNIV test autogyro that had been used for more than 15 years in autogyro's flight mechanics research studies. However, the G-UNIV mathematical model used in those studies are based on the individual-blade modelling approach, of which is mentioned in the UK's Civil Aviation Authority (CAA) report '*The Aerodynamics of Gyroplane*' (Anon., 2010). Employing a helicopter's multiblade modelling approach on the same autogyro in this particular research is briefly explained in the following.

THE ROTOR MODEL

The main rotor model is the most critical subsystem in a helicopter mathematical model since it is known as the subsystem that mainly contributes to the dynamic behaviour of the vehicle

during flight. The primary purpose of the main rotor subsystem in any helicopter mathematical model is to calculate the external load contributions of the rotor to the body-fixed axes set of the helicopter during flight. Taking the same concept on the rotor-disc of an autogyro, these external rotor loads are determined by first, calculating the absolute velocities and accelerations of the rotor *blade* through a sequence of kinematic transformations from the body axes frame in Eqs. (1) - (4) to the blade axes, as shown in Figs. 3 - 4. These kinematic transformations are also summarised through a simple flow chart in Fig.5, in which involving both, the *translational* and *rotational* (*angular*) components. The external forces and moments contribution of the rotor at the blade axes can then be determined from these local velocities and accelerations. These external loads are then transformed or translated back into the load contributions relative to the centre of gravity (body axes) of the autogyro, as described in the following sections.

Rotor Forces and Moments

The external forces contribution of the rotor blade can be obtained by considering the local aerodynamic and inertial forces acting at a point 'P' on the blade element as shown in Fig.6. The force per unit span at the local point is defined by

$$\boldsymbol{f}_P^{bl} = -m_0 a_x^{bl} \boldsymbol{i_{bl}} + \left(f_y^{bl} - m_0 a_y^{bl}\right)\boldsymbol{j_{bl}} + \left(f_z^{bl} - m_0 a_z^{bl}\right)\boldsymbol{k_{bl}} \tag{5}$$

where f_y^{bl} and f_z^{bl} are the local aerodynamic forces in the *y-blade* and *z-blade* direction at the local point and m_0 is the mass per unit span of the blade element. a_x^{bl}, a_y^{bl} and a_z^{bl} are the local blade element accelerations in the *x-blade*, *y-blade* and *z-blade* direction, acquired from the previous kinematic transformations. The elemental force f_x^{bl} is neglected as the blade is assumed to be rigid and fixed to the root of the rotor hub and rotating in the direction perpendicular to the *x-blade* axis.

The local aerodynamic load components of the blade element are also defined as the function of local tangential and normal airflow components (U_T and U_P) that flow through a 2-dimensional aerofoil, as shown in Fig. 7. These loads are analytically integrated across the radial distance of the blade and averaged along the azimuth blade position around the shaft, which represents a 'rotor disc' (refer to Fig. 8).

$$\boldsymbol{F}_A^{bl} = \begin{bmatrix} X_A^{bl} \\ Y_A^{bl} \\ Z_A^{bl} \end{bmatrix} = \frac{1}{2}\rho c \begin{bmatrix} 0 \\ \int_0^R \left(\delta U_T^2 - a_1 U_P U_T - a_0 U_P^2\right) dr_b \\ -\int_0^R \left(a_0 U_P U_T + a_1 U_T^2\right) dr_b \end{bmatrix} \tag{6}$$

In Eq. (6), $\boldsymbol{F}_A^{bl}$ is the aerodynamic force contributions in the blade axes, ρ is the local air

density, c is the blade chord length and δ is the average drag of the blade element. a_0 is the lift curve slope of the blade element and a_1 is the lift coefficient of the blade at zero angle of attack. R is the blade radius.

The loads are calculated in the form of force coefficients transmitted to the rotor shaft in the hub axes (C_x^h, C_y^h, C_z^h), and then transformed to the body axes through the shaft control angles (denoted as θ_s and ϕ_s). These external rotor force contributions are then written as

$$\begin{bmatrix} X_R^b \\ Y_R^b \\ Z_R^b \end{bmatrix} = \rho(\Omega R)^2 \pi R^2 \begin{bmatrix} C_x^h \cos\theta_s + C_y^h \sin\theta_s \sin\phi_s + C_z^h \sin\theta_s \cos\phi_s \\ C_y^h \cos\phi_s - C_z^h \sin\phi \\ -C_x^h \sin\theta_s + C_y^h \cos\theta_s \sin\phi_s + C_z^h \cos\theta_s \cos\phi_s \end{bmatrix} \tag{7}$$

where X_R^b, Y_R^b, Z_R^b are the translational rotor force contributions in the x, y and z-body axes.

For the rotor *moments*, it is determined by considering the elemental moment per unit span of the blade as the function of aerodynamic forces at local point P (referring back to Fig. 6), and expressed by

$$\boldsymbol{M}_R^{bl} = \int_0^R \Big(\boldsymbol{r}_{P/bl} \times \boldsymbol{f}_P^{bl}\Big) dr_b = Q_R^{bl} \tag{8}$$

where $\boldsymbol{f}_P^{bl}$ is the local blade element force vectors from Eq. (5), $\boldsymbol{r}_{P/bl}$ is the position vector of the blade element and Q_R^{bl} is the rotor torque in the blade axes.

The rotor blade of a light autogyro is actually a 'teetering' type, where flapping on one side of the blade tip causes the other side of the tip to flap in the opposite direction with the flapping angle β as shown in Fig. 8. Hence, this flapping angle is also known as the 'teetering angle' of the rotor disc, of which is unique for an autogyro case. Therefore, it is important to note that the control angles (θ_s and ϕ_s in Fig. 4) indicate only the shaft tilt angles and does not represent the actual rotor disc angle, of which is given by the additional function of flapping (teetering). These control shaft offset also contributes to the angular rates of the entire airframe, thus the rotor moment relative to the c.g.

Therefore, from the rotor forces calculated in Eq.(7), the total moment contributions of the rotor disc in the body axes set are solved from Eq. (8) and given by

$$\begin{bmatrix} L_R \\ M_R \\ N_R \end{bmatrix} = \begin{bmatrix} -Y_R\Big(x_{off} \sin\theta_s + z_{off} \cos\theta_s \cos\phi_s + z_{pcg}\Big) - Z_R\Big(z_{off} \sin\phi_s\Big) \\ X_R\Big(x_{off} \sin\theta_s + z_{off} \cos\theta_s \cos\phi_s + z_{pcg}\Big) - Z_R\Big(x_{pcg} - x_{off} \cos\theta_s + z_{off} \sin\theta_s \cos\phi_s\Big) \\ X_R\Big(z_{off} \sin\phi_s\Big) + Y_R\Big(x_{pcg} - x_{off} \cos\theta_s + z_{off} \sin\theta_s \cos\phi_s\Big) \end{bmatrix} \tag{9}$$

where L_R, M_R, N_R are the roll, pitch and yaw moment contributions of the rotor. x_{off} and z_{off} are defined as the offset location of the rotor hub from the pivot point, x_{pcg} and z_{pcg} are

location of the pivot point relative to the autogyro's c.g. (refer to Fig. 3 and 4).

The calculated external rotor disc forces and moments contribution relative to the autogyro's centre of gravity from Eq. (7) and (9) are then used in the complete autogyro model to determined the vehicle's dynamic responses. The trim simulation results of the autogyro model are shown in the model's validation.

VALIDATION OF THE MULTIBLADE ROTOR MODEL

The validation of the new autogyro model is made in the comparison between the model's simulation and the flight test data of the same autogyro acquired from the UK's Civil Aviation Authority (CAA) report 'The Aerodynamics of Gyroplanes' Anon. (2010). The autogyro data used in the research belongs to Montgomerie-Parsons G-UNIV test autogyro with configurations mentioned in Table 1.

The simulation results of the new autogyro model in comparison to the real flight test data are shown in Fig. 9. The results show the three flight states and two control parameters of the vehicle at trim condition. The trim condition in this context is referring to the flight condition where all forces and moments of the vehicle are in equilibrium, with zero rates of change in all three axes of rotations. The three flight states are the fuselage pitch and roll attitudes (denoted as Θ and Φ), and the rotorspeed (Ω). The two primary controls for the autogyro manoeuvre are the longitudinal and lateral controls, which are in the form of direct mechanical linkages between the control stick and the rotor shaft. Since the shaft is directly connected to the pivot point, the longitudinal control is physically addressed by the longitudinal tilt angle of the shaft about the *y-pivot* axis (θ_s), while lateral control is addressed by the lateral tilt about the *x-pivot* axis (ϕ_s). Again, Fig. 4 is referred to, for better clarity.

In general, the results show a good agreement between the model and the flight data for most parameters. The longitudinal parameters i.e. pitch attitude (Θ) and control (θ_s) responded by a decrease in values with the increment of forward velocities. These correlations are seen to be strong regarding the trend, as the calculation of the forces and moments of the subsystems are in the function of forward velocities and accelerations of the aircraft. As the forward velocity increases, the fuselage induced drag also increases, thus reduces the fuselage pitch angle. Correspondingly, the longitudinal shaft tilt also decreases with the increasing in forward velocity. Since the rotor disc tilted backwards in normal flight, the changes in forward velocity also contribute to more wind drag created at the rotor disc and eventually kills the lift due to turbulence behind the rotor disc. This longitudinal shaft tilt is reduced with the forward velocity to maintain a positive induced airflow through the rotor disc, thus maintaining the aerodynamic lift at trim flight.

The longitudinal tilt control (θ_s) and the rotorspeed (Ω) also indicate an average of less than twenty percent deviation from the flight data values. These are also expected when the multi-blade approach is employed in the rotor model, where the rotor loads are calculated as the average contribution of the blade elements throughout the whole span of the blade. The aerodynamic details of the blade element such as the lift and drag coefficients at different points on the blade and different Mach numbers are not modelled, which results in the detail rotor load contributions not captured in the calculations. Therefore, a more uniform pattern in the simulation than the flight data is also expected due to this.

The simulation results of the same autogyro were furnished in the same report (Anon., 2010), but was based on the 'individual-blade' rotor model. This model was originally used for helicopter simulations, but modified to suits for an autogyro simulations. The precise prediction of the model is undoubted as it had been used in numbers of autogyros flight dynamic studies as found in a number of references (Houston, 2000; Thomson and Houston, 2008, 2004; Houston and Thomson, 1995; Duda et al., 2011). However, the implementation of this individual-blade approach also associates with the computer run-time and hardware issues that became quite significant in the larger scale simulations.

CONCLUSIONS

Due to the unique flying principle an autogyro has as compared to a helicopter, employing a helicopter model for an autogyro involved several modifications, primarily on the rotor model, where the dynamic characteristics of the vehicle depended on. The autogyro simulation model employed in the CAA report (Anon., 2010) (where the flight test data were taken from) was based on the *individual-blade* approach, in which the blade element is extensively modelled, with a higher fidelity of results and closest to the flight data. However, the trim validation results of the *multiblade* autogyro model in this research indicate acceptable agreements with the flight data. The little drawback seen on the simulation results of the multiblade model are due to the limitations the multiblade approach has that contribute to the deviations in the results. This is due to the level of uncertainty associated with the multiblade modelling approach, in which the aerodynamic and geometrical characteristics of the rotor blade are not captured in detail. This small deviation can be seen as a modelling trade-off between the two approaches. Individual-blade approach contributes to better prediction results, but implementing it is cumbersome and less economical concerning to hardware and high simulation run-time. The multiblade model, however, is seen to be easier and more practical for a more complex and larger scale of application in simulations such as inverse simulations, flight stability and control enhancement, etc. Employing the multiblade rotor model on helicopter applications had well proven in various studies, and a few are mentioned here (Thomson, 1992; Ferguson and Thomson, 2015; Ferguson, 2015). Moreover, the reliability of the new autogyro multiblade model developed in this research had also proven, as the same model was employed on the inverse simulation study by Gallup

(2014). It is expected that more simulation results for autogyro related applications will be generated through the same modelling approach in the future.

REFERENCES

Anon. (2002). CAP 735 Aviation Safety Review 1992 - 2001. Technical report, Safety Regulation Group, Civil Aviation Authority.

Anon. (2010). The Aerodynamics of Gyroplanes. Technical report, CAA UK.

Bagiev, M. and Thomson, D. G. (2009). Handling Qualities Evaluation of an Autogiro Against the Existing Rotorcraft Criteria. *Journal of Aircraft*, 46(1):168–174.

Bagiev, M. and Thomson, D. G. (2010). Handling Qualities Assessment of an Autogiro. *Journal of the American Helicopter Society*, 55(3):032003.

Duda, H., Pruter, I., Deiler, C., Oertel, H., and Zach, A. (2011). Gyroplane Longitudinal Flight Dynamics. In *CEAS 2011 - The International Conference of the European Aerospace Societies*.

Ferguson, K. (2015). *Towards a Better Understanding of the Flight Mechanics of Compound Helicopter Configurations*. Phd, University of Glasgow.

Ferguson, K. and Thomson, D. (2015). Flight Dynamics Investigation of Compound Helicopter Configurations. *Journal of Aircraft*, 52(1):156–167.

Gallup, M. (2014). Inverse Simulation of Autogyros. Technical Report August, University of Glasgow.

Houston, S. (1991). *Rotorcraft aeromechanics simulation for control analysis: mathematical model description*. Internal report. University of Glasgow, Department of Aerospace Enginnering.

Houston, S. and Thomson, D. (1995). A Study of Gyroplane Flight Dynamics. In *21st European Rotorcraft Forum*, number Paper No. VII-6, St. Petersburg, Russia. ERF1995.

Houston, S. S. (2000). Validation of a rotorcraft mathematical model for autogyro simulation. *Journal of Aircraft*, 37(3):403–409.

Leishman, J. G. (2006). *Principles of Helicopter Aerodynamics*. Cambridge University Press.

Padfield, G. D. (2008). *Helicopter Flight Dynamics (Google eBook)*. John Wiley & Sons, 2nd ed. edition.

Thomson, D. and Houston, S. (2004). Experimental and Theoretical Studies of Autogyro Flight Dynamics. In *(ICAS 2004) 24th Congress of International Council of the Aeronautical Sciences*, Yokohama.

Thomson, D. and Houston, S. (2008). Advances in the Understanding Autogyro Flight Dynamics. In *64th American Helicopter Society Annual Forum*, number April, pages 391–403, Montreal, Canada. AHS International, Inc.

Thomson, D. G. (1992). Development of a Generic Helicopter Model for Application to Inverse Simulation. Technical Report 9216, University of Glasgow, Glasgow.

Table 1: Montgomerie-Parsons GUNIV Autogyro Configurations

Parameter	Value
Gross Mass (m)	355 kg
Moments of Inertia:	
I_{xx}	72.96 $kg\,m^2$
I_{yy}	297.21 $kg\,m^2$
I_{zz}	224.25 $kg\,m^2$
I_{xz}	0 $kg\,m^2$
Rotor Parameters:	
Radius (R)	3.81 m
Chord (c)	0.197 m
Rotor Mass (m_r)	17.255 kg
Lift Curve Slope (a_0)	$5.75/rad$

Fig. 1: Montgomerie-Parsons G-UNIV Research Autogyro

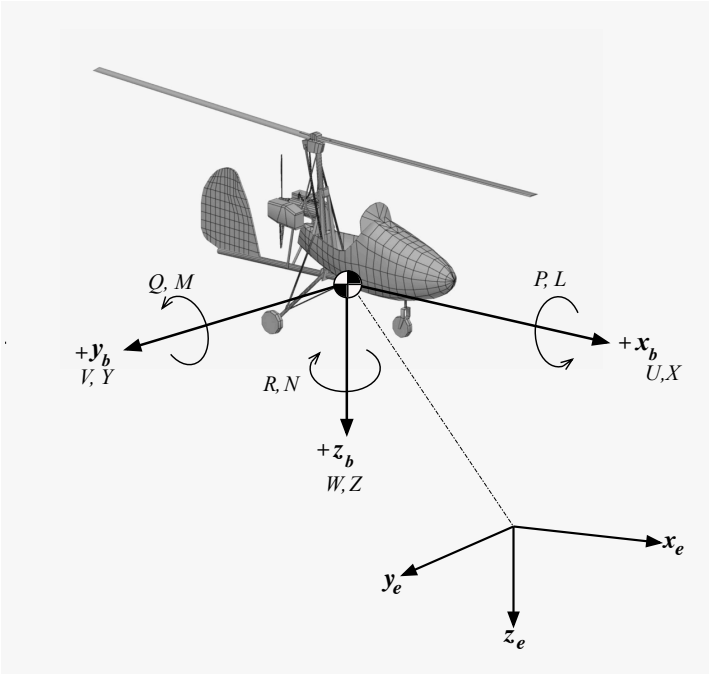

Fig. 2: Autogyro body and earth references

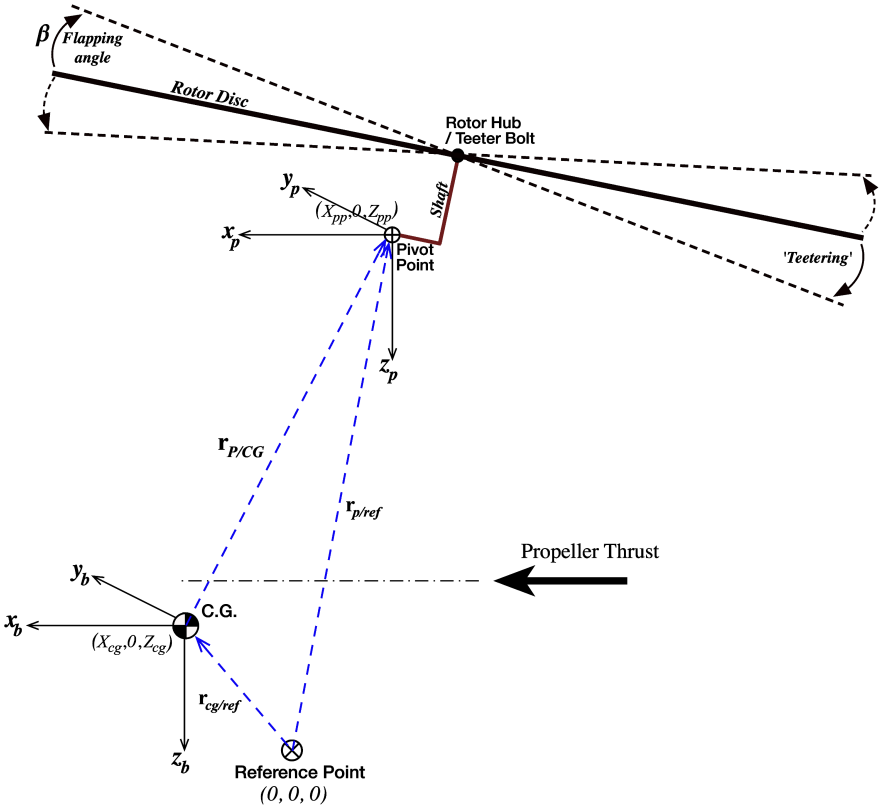

Fig. 3: The transformations from the body axes to the hub axes of a light autogyro

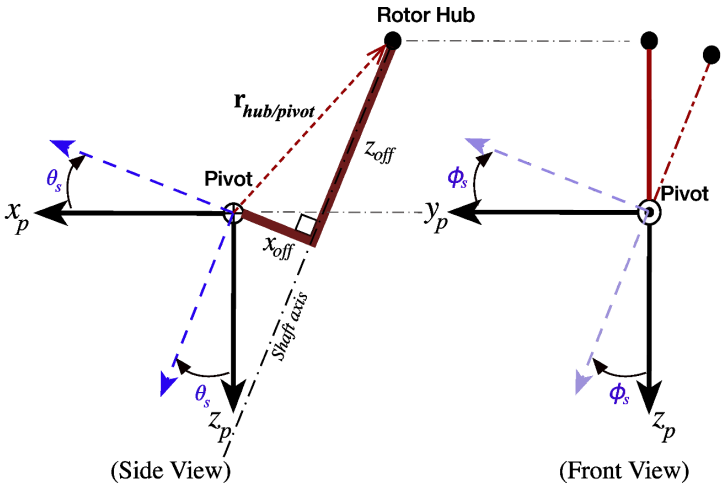

Fig. 4: The longitudinal and lateral control angles

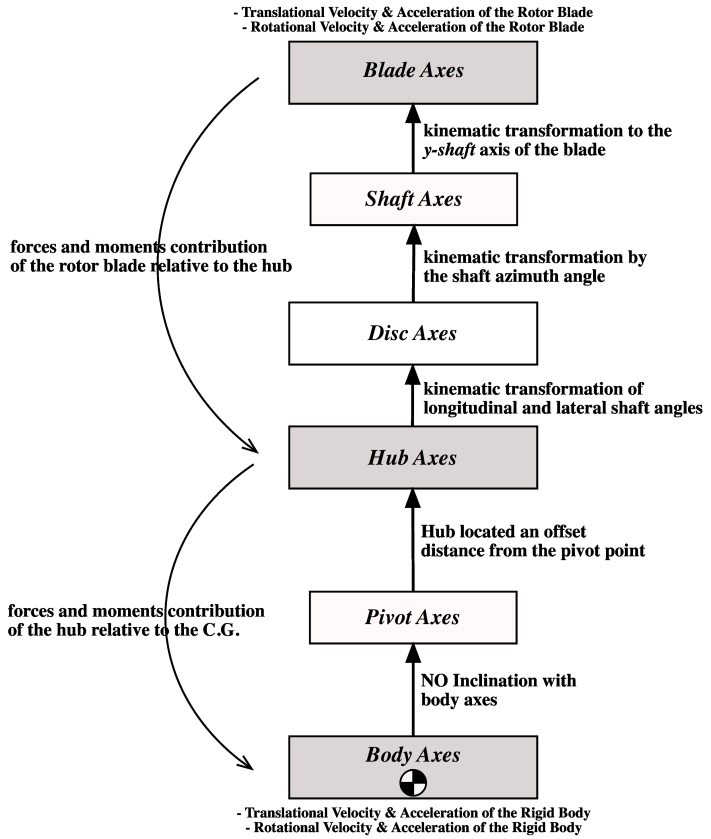

Fig. 5: Flow chart of transformations between the body axes and the blade axes of the autogyro

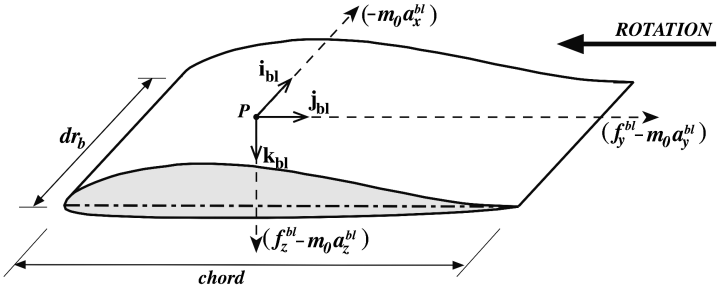

Fig. 6: Forces on a Blade Element

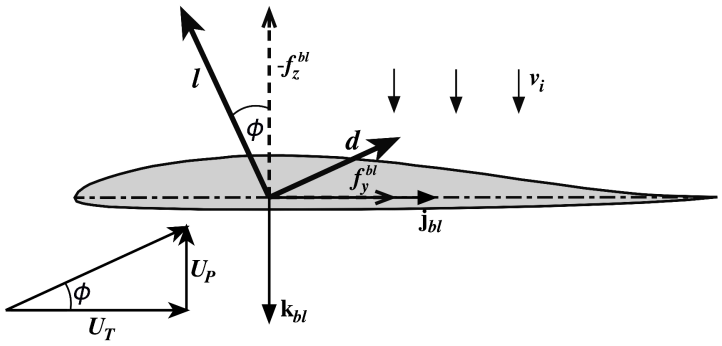

Fig. 7: The blade element's normal and tangential velocity components (angle exaggerated for clarity)

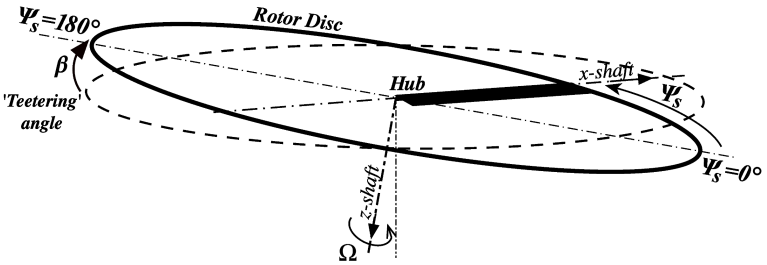

Fig. 8: Blade rotation with respect to the azimuth position

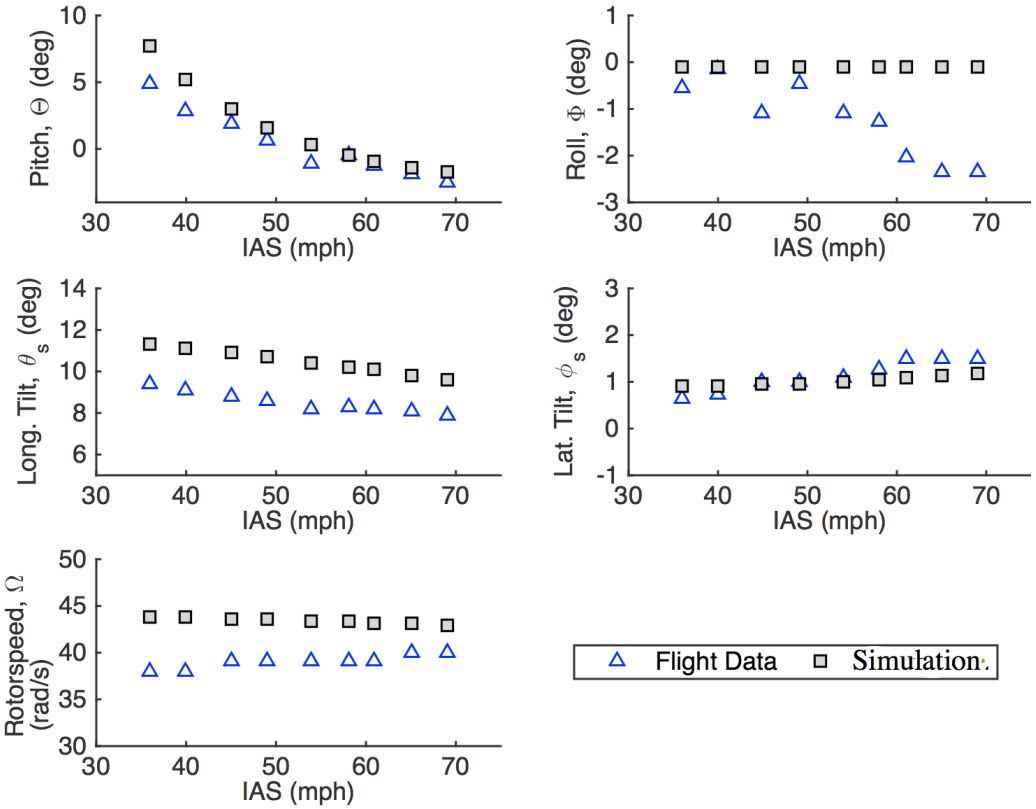

Fig. 9: Trim flight comparison with real flight data